Contents lists available at ScienceDirect

Systems & Control Letters

journal homepage: www.elsevier.com/locate/sysconle



Flocks, games, and cognition: A geometric approach[★]

Udit Halder ^{a,1}, Vidya Raju ^{b,1,2}, Matteo Mischiati ^c, Biswadip Dey ^d, P.S. Krishnaprasad ^{e,*}



- a Coordinated Science Laboratory, University of Illinois, Urbana-Champaign, IL 61801, USA
- ^b John A. Paulson School of Engineering and Applied Sciences, Harvard University, MA 02138, USA
- c OM1 Inc., Boston, MA 02116, USA
- d Siemens Corporation, Technology, Princeton, NI 08540, USA
- e Institute for Systems Research and Department of Electrical and Computer Engineering, University of Maryland, College Park, MD 20742, USA

ARTICLE INFO

Article history:
Received 5 August 2022
Received in revised form 31 December 2022
Accepted 15 February 2023
Available online xxxx

Keywords: Flock behavior Energy modes Evolutionary game Cognitive cost

ABSTRACT

Avian flocks display a wide variety of flight behaviors, including steady directed translation of center of mass, rapid change of overall morphology, re-shuffling of positions of individuals within a persistent form, etc. These behaviors may be viewed as flock-scale *strategies*, emerging from interactions between individuals, accomplishing some collective *adaptive* purpose such as finding a roost, or mitigating the danger from predator attacks. While we do not conceive the flock as a single cognitive agent, the moment-to-moment decisions of individuals, influenced by their neighbors, appear *as if* to realize collective strategies that are cognizant of purpose. In this paper, we identify the actions of the flock as allocation of energetic resources, and thereby associate a *cognitive cost* to behavior. Our notion of cognitive cost is a measure of the temporal variability of such resource allocation. Using a recently developed natural geometric approach to kinetic energy allocation, we map the flock behavior to a temporal signature on the standard (probability) simplex. From the signature of a flocking event, we calculate the cognitive cost as a solution to an optimal control problem based on a game-theoretic model. Alternatively, one can associate to a signature an *entropic cost*. These two cost measures, when applied to data on starling flocks, show a consistent spread in value across events, and we suggest the possibility that higher cost may arise from flock response to predator attacks.

© 2023 Elsevier B.V. All rights reserved.

1. Introduction

In modern studies of avian flocks, significant progress has been made, thanks to advances in motion capture technologies based on computer vision, as in the work of Cavagna and collaborators [1–4], and GPS data-logging methods as in the work of Vicsek and collaborators [5]. While the investigations of starling flocks in [1,2] were focused on the structure and statistics of interactions ruling the observed flocking events (a bottom-up approach), questions of flock-scale phenomena, such as information transfer through waves were the subject of [3,4,6]. In [5] the

E-mail address: krishna@umd.edu (P.S. Krishnaprasad).

authors were concerned with pigeon flocks engaged in free flight or homing behaviors and the appearance of leadership structures in these settings. In this paper, we are concerned with flockscale phenomena found in the starling flight data obtained by the Collective Behavior in Biological Systems (COBBS) group, led by Dr. Andrea Cavagna and Dr. Irene Giardina of the Institute for Complex Systems (ISC-CNR) in Rome, Specifically, we use a top-down approach to the dynamics of observed flight behaviors, including steady directed translation of center of mass of the flock, rapid change of overall morphology, re-shuffling of positions of individuals within a persistent form, etc. It has been suggested that such behaviors confer anti-predatory advantage on flocks thanks to the confusion effect [7-11] - predators such as peregrine falcons, that are exceptionally successful with isolated targets, are foiled by the perceptual challenges posed by large flocks [12]. The time course of fractional allocation of kinetic energy resource among different behaviors can be represented as a signature of a flocking event on a standard simplex. Treating distinct flight behaviors as competing pure strategies in a game, the signature is a trace of mixed strategies. We draw on the subject of evolutionary game theory to establish natural families of dynamics and control systems on the simplex. Fitting a generative model from such a family to each signature is formulated

This research was supported by the Air Force Office of Scientific Research under AFOSR, USA Grant FA9550-10-1-0250, an AFOSR, USA FY2012 DURIP Grant No. FA2386-12-1-3002, the ARL/ARO MURI Program, USA Grant No. W911NF-13-1-0390, through the University of California Davis (as prime), the ARL/ARO, USA Grant No. W911NF-17-1-0156, through the Virginia Polytechnic Institute and State University (as prime), the National Science Foundation, USA CPS: Medium Grant CNS-2013824 through University of California Irvine (as prime), and by Northrop Grumman Corporation, USA.

^{*} Corresponding author.

¹ Equal contributions.

² Currently at Tandon School of Engineering, New York University.

as an optimal control problem on the simplex. Solutions to such optimal control problems allow us to propose and examine a notion of cognitive cost of flock behavior.

Computer vision algorithms yield data on starling flocks in the form of streams of three dimensional coordinates of individuals in a flocking event approximately every 6ms [3,13]. To extract dynamical properties of trajectories, including velocity and acceleration, it is necessary to smooth the data. While there is a long history of smoothing techniques in biological data analysis, we used an efficient method based on the theory of optimal control of linear systems with quadratic cost functionals, to obtain smoothed trajectories for each bird [14,15]. The passage from individual-scale to flock-scale analysis is based on a recent development of the idea of kinematic modes in many-particle systems [16]. Using the geometric language of fiber bundles, the velocity of the flock as a whole is split into several mutually orthogonal components (kinematic modes). The notion of orthogonality is based on a Riemannian metric tensor defined by the masses of individuals (here assumed to be equal on the basis of homogeneity of the flock). We note that our kinematic modes are akin to the chemist's idea of normal modes of vibration of polyatomic molecules in spectroscopy [17–19]. The kinetic energy of a flock is in turn split into energy modes (e.g. kinetic energy relative to center of mass, and its further splitting into kinetic energy of flock shape deformation relative to center of mass, kinetic energy of global rigid rotation etc.). Taking fractions of the different energy modes with respect to the kinetic energy relative to center of mass yields a signature of a flocking event on a standard (probability) simplex. In [16] this process was applied to pigeon flock data from [5] purely as an application of the computation of energy modes.

The simplex is the natural space for representing mixed strategies in a game with finitely many pure strategies [20]. In a typical flocking event one does not see sustained pure strategies e.g. global rigid rotation. Instead one finds non-zero fractions of multiple energy modes, which we interpret as the occurrence of mixed strategies. In the development of evolutionary game theory in biology [21], a central idea is that of replicator dynamics [22,23] specified by a vector-valued fitness map on the simplex. It captures the evolution of mixed strategies. In a recent development [24,25], it has been suggested that such dynamics may be viewed as occupying the middle layer of a three layer cognitive hierarchy where the top (cognitive) layer concerns the control of replicator dynamics through modulation of fitness maps. This is of particular interest, since the observed signature of a flocking event cannot in general be identified with a fixed replicator dynamics due to self-intersections, but one can fit a controlled replicator dynamics to the signature. The control enables time-dependence of energy mode allocation. This leads to a natural optimal control problem on the simplex, to be solved by construction of a Hamiltonian system via the Maximum Principle of Pontryagin and coworkers [26]. The time-averaged Hamiltonian arising from the optimal solution directly reflects the rate of re-allocation of energy resource among different energy modes. For this reason, we interpret the time-averaged Hamiltonian as cognitive cost of flocking. On the other hand one can associate an entropy value to each point on a signature curve, and hence the average entropy of the signature. This reflects the degree of unpredictability of flock behavior and the extent of confusion effect that a predator targeting a flock is subject to. This measure is insensitive to the temporal variation of the flock signature. This paper examines both these measures on starling flock data. In what follows, we discuss the organization and contributions of this paper.

In Section 2, we briefly indicate the characteristics of the starling flock data used in this paper. Section 3.1 is an account

of the linear-quadratic optimal control methods [14.15] used to smooth the sampled data to obtain trajectories of individual birds in the flocking events. In Section 3.2, a brief summary of a more general approach based on the Pontryagin Maximum Principle (PMP) is given for use later in Section 5.2 in connection with the optimal energy mode allocation problem. In Section 4 the different energy mode splittings originating in [16] are described. Section 5 provides an outline of the concept of cognitive hierarchy developed in [24] and specializes it in Section 5.1 to the setting of games with two pure strategies. This leads to the optimal control problem in the cognitive layer discussed in Section 5.2. The resulting evaluations of cognitive cost and entropic cost under energy splittings for eight flocking events are presented and compared in Section 6. The value of such measures lies in ordering or distinguishing flocking events, with the possibility of discerning/suggesting underlying causes for the observed differences. We conclude with discussions and interpretations of these results in Section 7.

Historical Remark: The cognitive cost of human decision-making has been of interest to researchers in behavioral psychology and neuroscience for quite some time (see [27] and references therein, as well as [28]). In [27], a combination of physiologically plausible models of glycogen metabolism in the brain, an associated optimal control formulation, and simulation experiments are used to put forward a case for energy utilization as a means to account for cognitive cost. While this presupposes that the brain has an intelligent control system to manage the use of its metabolic resources, in the present work we do not wish to suggest any sort of central authority controlling resource allocation in the flock. Indeed one expects that the energy resource (mode) allocation, seen in starling data is an epiphenomenon of perceptually-guided steering behaviors of individuals responding to conspecific neighbors and predators (such as peregrine falcons). Individual behaviors may have been selected through evolution thanks to the benefits of predator avoidance conferred by flock-scale behaviors that engender the confusion effect. While the notion of energy resource allocation in our work parallels that in [27], we are not dependent on any physiologically based models. Instead our measure of cognitive cost is centered on: (i) it is possible to recognize a finite set of flock-scale behaviors; (ii) there are associated kinetic energy modes; and (iii) rapid resource reallocation across energy modes (modeled via controlled replicator dynamics) incurs a burden (measured as cognitive cost using optimal control theory). In the investigation of signatures of decision-making processes, cognitive scientists have identified a spectrum ranging from the automatic, fast, and relatively inflexible extreme to the slower, flexible, and deliberative extreme, the latter often referred to as "cognitive control" - a term we do not use in this paper to avoid conflating with control-theoretic usage [29]. It is important to note that these authors initiate and explore a modeling approach based on replicator dynamics on the 1-dimensional simplex, incorporating various feedback laws, and costs. The fast and slow extremes are treated as pure strategies in a game, akin to the notion of energy modes (with mechanical origins) in our own work. As we show later, the geometric approach of the present work allows consideration of signatures in higher dimensional simplices. Another relevant antecedent for our control-theoretic notion of cognitive cost has to do with the problem of selective attention to sensory input and motor sequences - of great interest to neuroscience and cognitive science. In pioneering work Roger Brockett formulated a notion of cost of attention, which leads to novel problems of infinite dimensional control - specifically (optimal) control on the diffeomorphism group and Liouville equations [30].

Whereas this paper is aimed at quantitative exploration of flocking events and their dynamic morphologies by considering underlying adaptive purpose (e.g. predation avoidance), the recorded history of observations by naturalists have for long provided questions and suggested qualitative explanations that have stimulated research. In her article [31], referring to the naturalist Edmund Selous as a confirmed Darwinian, Margaret Nice quotes from his famous book [32] this memorable description (on page 141) of a starling flock:

"...and now, more and faster than the eye can take it in, band grows upon band, the air is heavy with the ceaseless sweep of pinions, till, glinting and gleaming, their weary wayfaring turned to swiftest arrows of triumphant flight—toil become ecstasy, prose an epic song—with rush and roar of wings, with a mighty commotion, all sweep, together, into one enormous cloud. And still they circle; now dense like a polished roof, now disseminated like the meshes of some vast all-heaven-sweeping net, now darkening, now flashing out a million rays of light, wheeling, rending, tearing, darting, crossing, and piercing one another —a madness in the sky".

In this passage one senses the fascination that the dynamic flock morphology and its likely purpose hold for casual and scholarly observers alike. Further on Selous speculates about the collective guidance that might drive the phenomenon (pages 142–143 in [32]). A modern view treats the phenomenon as the result of co-evolution of predator (peregrine falcon) and prey (common starling) – to quote naturalist Grainger Hunt [12]:

"What are we to make of the pulsating, other-worldly spectacle of a massive starling flock, moving amoeba-like across the open skies? A Peregrine Falcon or other winged predator is almost always involved, as the thousands of individual flock members fight to evade capture".

And again,

"The wondrous cloud [of starlings] is thus secondary – an extraneous property, emerging from independent attempts by each individual, within the multitude of self-interested starlings, to escape the falcon". [12]

Hunt also views as a relevant factor the self-interest of the falcon in avoiding injury that might result from even a grazing collision with a starling in a flock – thereby raising the failure rate for prey-capture by the falcon.

"And so the peregrine attacks the flock gingerly, and in apparent moderation of its true ability to catch [an isolated] starling". [12]

Contributions of this paper: This paper presents a new integrative treatment of avian flocking behavior by bringing together computational tools, optimal control theory, evolutionary game dynamics, and geometric decompositions to shed light on the question - is there a quantitative mechanism, for ordering of flocking events that exhibit dynamic morphology, that is consistent with the idea that a purpose of flocking is to mitigate predation risk? This problem is framed here as a game with finitely many discrete strategies (flock behaviors), which are identified with energy modes derived from geometric decompositions of flock-scale kinematics. Until now discrete flock behaviors have been understood in terms of qualitative observer-dependent categorizations (e.g. a flock displaying Wave events, Blackening, Flash expansion, Vacuole, Split into subflocks, Merge of multiple subflocks, Cordon, Flock dilution etc.) as in [11]. The dynamic probabilistic mixture of energy modes in data used in our paper naturally presents a signature of a flocking event on the probability simplex. Arguing that it is the temporal variability of the signature that matters for the ordering we seek, we use optimal control theory on the simplex to extract a measure of such variability for each event. Since this new measure (here called cognitive cost) signifies how big a perceptual/cognitive challenge an event is for a predator, we propose that it is an ordering mechanism – events that display high cognitive cost are more likely to have been induced by predator attacks resulting in flock behavior to counter the same. Using optimal control computations on individual trajectory data, and on flocking event signatures, we are able to present this new ordering mechanism, in contrast to the mainly qualitative and observer-dependent understanding from video data as in [11]. This is a key advance in our paper.

Matters outside the scope of this paper: We note that in this paper, we have not considered what may be viewed as countermeasures evolved by the predator (as in [33]) to *avoid* the confusion effect, nor have we taken account of the physiological aspects of bird vision [34], both likely to affect cognitive cost. Further, collective behavior in avian flocks may be shaped by purpose other than mitigation of predation risk. For consideration of this see the recent wide-ranging perspective article [35].

Dedication: We dedicate this paper to Professor Arthur Krener on his eightieth birthday, celebrating his many contributions to nonlinear and optimal control, geometric perspectives, and computational investigation.

2. Flocking data

This project grew out of a collaborative project funded by the U.S. Air Force Office of Scientific Research during the period 2010–2014, between the University of Maryland (Principal Investigator: P. S. Krishnaprasad) and the sub-awardee COBBS group (Co-Principal Investigator: Andrea Cavagna) at the Institute for Complex Systems in Rome (ISC-CNR), located at the University of Rome "La Sapienza". Andrea Cavagna had already pursued an earlier campaign of observations of starling flocks (with support from the European Union, StarFlag 2007).

Starlings gather around urban areas during winter months to gain extra warmth from the cities. They spend the day feeding in the countryside, and before settling on the trees for the night they gather in flocks to perform elaborate aerial displays. Data on flocking events were captured by the COBBS group (principally by researchers, Stefania Melillo, Leonardo Parisi, and Massimiliano Viale) between November 2010 and December 2012. Three high speed cameras (IDT M5) were used for this purpose, with a maximum frame rate of 170 frames per second (fps) at a resolution of 2288 ×1728 pixels. Data were collected at the site of Piazza dei Cinquecento in Rome near one of the major roosting sites used by starlings. Further details on the data collection instrumentation and signal processing can be found in the Methods Section (page 695) of [3]. Data pertaining to eight flocking events were supplied by Andrea Cavagna to the Maryland group (specifically P. S. Krishnaprasad). The details for the particular flocking events used in this paper are to be found in Table 1.

The data supplied to the Maryland group contained timestamped 3D coordinates of each bird in each flocking event, obtained using advanced computer vision algorithms developed by the COBBS group. One of the key steps in our analysis is to develop from this data, requisite trajectory characteristics at finer resolution through a process of smoothing discussed in the next section. In particular, velocity, acceleration and jerk were extracted in this way.

The flocking data came unlabeled in that none of the eight events was identified as occasioned by a predator attack even though starling flocks invariably elicit attention from peregrine falcons [12]. Our analysis below suggests candidate events that may be so labeled.

3. Data smoothing

Given a time-indexed sequence of sampled observations on a manifold, generative models provide a meaningful way of capturing them through the use of an underlying dynamical system complete with control inputs having useful interpretations. The control inputs are determined by solving an optimal control problem, where the cost function consists of a data-fitting term that penalizes mismatch between the generated trajectory and sampled data, and a smoothing term weighted by a parameter λ that affects the smoothness of the generated trajectory. We discuss two generative models to solve this problem.

3.1. A linear generative model

A first approach to solving the data smoothing problem (in 3 dimensions), presented in [14], is to formulate an optimal control problem to minimize the jerk path integral, with intermediary state costs determining the fit error. Suppose that $\{\mathbf{r}_i\}_{i=0}^N$ denote the positions $\mathbf{r}_i \in \mathbb{R}^3$ of the birds at each sampling time instant t_i . In order to recover a trajectory fit $\mathbf{r}(t):[t_0,t_N]\to\mathbb{R}^3$, one can use the jerk-driven linear generative model

$$\dot{\mathbf{r}}(t) = \mathbf{v}(t)
\dot{\mathbf{v}}(t) = \mathbf{a}(t)
\dot{\mathbf{a}}(t) = \mathbf{u}(t),$$
(1)

where $\mathbf{v}(t)$, $\mathbf{a}(t)$, $\mathbf{u}(t)$ denote the velocity, acceleration, and jerk (input) of the trajectory respectively. The cost functional to be minimized is

$$J_{l} = \sum_{i=0}^{N} \|\mathbf{r}(t_{i}) - \mathbf{r}_{i}\|^{2} + \lambda \int_{t_{0}}^{t_{N}} \|\mathbf{u}(t)\|^{2} dt,$$
 (2)

where $\|\cdot\|$ denotes the Euclidean norm, and the minimization is over initial conditions $\mathbf{r}(t_0)$, $\mathbf{v}(t_0)$, $\mathbf{a}(t_0)$ and the input function $\mathbf{u}(\cdot)$. Defining the state as

$$\mathbf{x}(t) = \begin{bmatrix} \mathbf{r}(t) \\ \mathbf{v}(t) \\ \mathbf{a}(t) \end{bmatrix} \in \mathbb{R}^9, \tag{3}$$

we can write (1) as the linear control system

$$\dot{\mathbf{x}}(t) = A\mathbf{x}(t) + B\mathbf{u}(t),\tag{4}$$

with the matrices A and B defined appropriately. The problem of minimizing J_l subject to (4) becomes a linear, quadratic optimal control problem, which can be solved by a completion of squares of terms in the cost by invoking a path independence lemma, or by applying the Pontryagin Maximum Principle as shown in [14]. This approach has been used to smooth the starling flock data [15] for all the events listed in Table 1, with the parameter λ found by leave-one-out cross validation.

3.2. Data smoothing in the Euclidean setting

subject to: $\dot{x} = f(x, u)$

In this section, we present a general result on the Pontyagin Maximum Principle based approach for data smoothing on the Euclidean space \mathbb{R}^k . Suppose that $\left\{x_i^d\right\}_{i=0}^N$ denote the sampled data. For a generative model given by the dynamics $\dot{x}=f(x,u)$ on \mathbb{R}^k , with the control $u\in\mathbb{R}^m$, the optimal control problem can be formulated as

$$\min_{x(t_0), \ u(\cdot)} J(x(t_0), u) = \sum_{i=0}^{N} F_i(x(t_i), x_i^d) + \frac{\lambda}{2} \int_{t_0}^{t_N} \|u(t)\|^2 dt,$$
 (5)

Table 1Details of captured flocking events.

Flocking Event	Flock size (n)	Duration (seconds)	Data capture rate (frames/second)
1	175	5.4875	80
2	123	1.8176	170
3	46	5.6118	170
4	485	2.3471	170
5	104	3.8824	170
6	122	4.1588	170
7	380	5.7353	170
8	194	1.7588	170

where parameter $\lambda > 0$ is a regularization parameter, and F_i 's are suitably defined *fit errors* of the reconstructed trajectories and sampled data at the sampling times. Using Pontryagin Maximum Principle, the optimal control values can be calculated as a function of the state and a co-state variable. The following result from [36] states this precisely.

Theorem 3.1 (PMP for Data Smoothing [36]). Let $u^*(\cdot)$ be an optimal control input for (5), and let $x^*(\cdot)$ denote the corresponding state trajectory. Then there exists a costate trajectory $p:[t_0,t_N]\to\mathbb{R}^k$, $p\neq 0$, such that

$$\dot{x}^* = \frac{\partial \mathcal{H}}{\partial p}(t, x^*, p, u^*)
\dot{p} = -\frac{\partial \mathcal{H}}{\partial x}(t, x^*, p, u^*),$$
(6)

during $t \in (t_i, t_{i+1}), \ i = 0, 1, \dots, N-1$, and the Hamiltonian is given as

$$\mathcal{H}(t, x^*, p, u^*) = \max_{u \in \mathbb{R}^m} H(t, x^*, p, v), \tag{7}$$

for $t \in [t_0, t_N] \setminus \{t_0, t_1, \dots, t_N\}$, where the pre-Hamiltonian is defined as $H(t, x, p, u) = p^T f(x, u) - \frac{\lambda}{2} \|u\|^2$. Moreover, jump discontinuities of the costate variable can be written as

$$p(t_0^-) = 0,$$

$$p(t_i^+) - p(t_i^-) = \frac{\partial F_i(x(t_i))}{\partial x(t_i)}, \quad i = 0, 1, \dots, N,$$

$$p(t_N^+) = 0.$$
(8)

The piecewise continuous nature of the co-state trajectory due to jump conditions arising from mismatch between the sampled data points and the reconstructed state must be noted here. The initial condition $x(t_0)$ is identified by using the terminal condition for the co-state, while the optimal value of λ is typically obtained through leave-one-out cross validation. The reconstructed trajectory is then obtained as the projection onto the state space of the solution of Hamilton's equations derived from the (maximized pre-) Hamiltonian. We refer the reader to [15] for a detailed treatment of this problem. This is the result that will be used in our data fitting problem on a simplex (Section 5.2).

4. Energy modes

Avian flocks display a variety of flight behaviors that may be characterized as collective strategies such as steady translation of center of mass (which we denote by com), coherent rotation about center of mass (rot), change of ensemble form (ens), internal re-shuffling of relative positions or democratic strategy (dem), (rapid) expansion or contraction of volume (vol) etc. A flocking event may display all of the mentioned strategies to varying degrees as governed by the time-dependent allocation of kinetic energy to each strategy. We take the viewpoint presented

in [16] and study the fractions of the total kinetic energy of a flock allocated to several 'kinematic modes' – rigid translations, rigid rotations, inertia tensor transformations, expansion and compression, in order to describe collective behavior. By doing so, we treat the flock as a single entity with several strategies of energy allocations emerging from individual behavior. Below is a brief discussion on the resolution of kinetic energy into components, from [16].

If the positions of the birds in a flock are denoted by $\{\mathbf{r}_1, \mathbf{r}_2, \dots, \mathbf{r}_n\}$, the center of mass can be written as

$$\mathbf{r_{com}} = \frac{1}{n} \sum_{i=1}^{n} \mathbf{r}_i,\tag{9}$$

where we treat every bird alike, i.e. their masses are taken to be equal to 1. The *ensemble inertia tensor* is defined by

$$K = \sum_{i=1}^{n} (\mathbf{r}_i - \mathbf{r}_{com}) (\mathbf{r}_i - \mathbf{r}_{com})^{\mathsf{T}}.$$
 (10)

Let the velocities of the birds be denoted as, $\{\mathbf{v_{r1}}, \dots, \mathbf{v_{rn}}\}$, then the total kinetic energy is

$$E = \frac{1}{2} \sum_{i=1}^{n} \|\mathbf{v_{ri}}\|^{2}. \tag{11}$$

We can define the position and velocity vector with respect to the center of mass, i.e. $\mathbf{c} \triangleq [\mathbf{c}_1, \dots, \mathbf{c}_n] \in \mathbb{R}^{3 \times n}$, where $\mathbf{c}_i = \mathbf{r}_i - \mathbf{r}_{\text{com}}$; $\mathbf{v}_{\mathbf{c}} \triangleq [\mathbf{v}_{\mathbf{c}1}, \mathbf{v}_{\mathbf{c}2}, \dots, \mathbf{v}_{\mathbf{c}n}] \in \mathbb{R}^{3 \times n}$, where $\mathbf{v}_{\mathbf{c}i} = \mathbf{v}_{\mathbf{r}i} - \mathbf{v}_{\mathbf{com}}$. Then

$$E_{\text{com}} = \frac{n}{2} \|\mathbf{v_{com}}\|^2, \quad E_{\text{rel}} \triangleq \frac{1}{2} \sum_{i=1}^{n} \|\mathbf{v_{ci}}\|^2.$$
 (12)

We thus have the splitting, $E = E_{\text{com}} + E_{\text{rel}}$. As shown in [16], instantaneous relative energy allocations can be expressed on the probability simplex, $^2 \Delta^4$ by exploiting two distinct fiber bundle structures of the flock's total configuration space to split the total kinetic energy using (i) ensemble fibration or (ii) shape fibration.

(i) Ensemble Fibration: We note that the ensemble inertia tensor K (10) is (for a generic flock configuration) a symmetric positive definite matrix. Hence its eigendecomposition can be written as, $K = Q \Lambda Q^{\mathsf{T}}$, with $\Lambda = \mathrm{diag}(\lambda_1, \lambda_2, \lambda_3)$, where $\lambda_1 \geq \lambda_2 \geq \lambda_3 > 0$. Define, $F := \mathbf{cv_c^{\mathsf{T}}} + \mathbf{v_c c^{\mathsf{T}}}$ and $\tilde{F} = [\tilde{F}_{ij}] = Q^{\mathsf{T}} F Q$. Then the following energy modes can be calculated

$$E_{\text{ens.rot}} \triangleq \frac{1}{2} \left(\frac{\tilde{F}_{12}^2}{\lambda_1 + \lambda_2} + \frac{\tilde{F}_{13}^2}{\lambda_1 + \lambda_3} + \frac{\tilde{F}_{23}^2}{\lambda_2 + \lambda_3} \right),$$

$$E_{\text{ens.def}} \triangleq \frac{1}{8} \left(\frac{\tilde{F}_{11}^2}{\lambda_1} + \frac{\tilde{F}_{22}^2}{\lambda_2} + \frac{\tilde{F}_{33}^2}{\lambda_3} \right).$$
(13)

Furthermore,

$$E_{\text{vol}} \triangleq \frac{1}{2} \frac{\text{tr}^2 \left(\mathbf{c} \mathbf{v}_{\mathbf{c}}^{\mathsf{T}} \right)}{\text{tr}(K)},\tag{14}$$

so that, $E_{\rm ens,res} = E_{\rm ens,def} - E_{\rm vol}$. We may also calculate $E_{\rm dem} = E_{\rm rel} - E_{\rm ens,rot} - E_{\rm ens,def}$. For interpretations of these energy modes, see [16]. (The notation $E_{\rm dem}$ in [16] is inspired by association with the term *democracy* transformation in [19].)

$$\Delta^{k-1} = \left\{ x = (x_1, x_2, \dots, x_k) \in \mathbb{R}^k : 0 \le x_i \le 1, \sum_{i=1}^k x_i = 1 \right\}.$$

Hence, in this fibration we have the following splitting of the kinetic energy

$$\left(\frac{E_{\text{com}}}{E}, \frac{E_{\text{dem}}}{E}, \frac{E_{\text{ens.rot}}}{E}, \frac{E_{\text{vol}}}{E}, \frac{E_{\text{ens.res}}}{E}\right) \in \Delta^4.$$
 (15)

(ii) *Shape Fibration*: Define the flock angular momentum, respectively the locked moment of inertia tensor, by

$$\mathbf{J} = \sum_{i=1}^{n} (\mathbf{c}_{i} \times \mathbf{v}_{\mathbf{c}i}),$$

$$I_{\mathbf{c}} = \sum_{i=1}^{n} (\|\mathbf{c}_{i}\|^{2} \mathbb{1} - \mathbf{c}_{i} \mathbf{c}_{i}^{\mathsf{T}}).$$
(16)

Then the rotational energy E_{rot} can be calculated as

$$E_{\text{rot}} \triangleq \frac{1}{2} \mathbf{J}^{\mathsf{T}} I_{\mathbf{c}}^{-1} \mathbf{J},\tag{17}$$

The shape residual energy is given by $E_{\rm shp,res} = E_{\rm rel} - E_{\rm rot} - E_{\rm ens,def}$, which provides the splitting in this fibration as below

$$\left(\frac{E_{\text{com}}}{E}, \frac{E_{\text{rot}}}{E}, \frac{E_{\text{shp.res}}}{E}, \frac{E_{\text{vol}}}{E}, \frac{E_{\text{ens.res}}}{E}\right) \in \Delta^4.$$
 (18)

While we can split the kinetic energy in 5 different modes (15), (18), many flocking events show a predominant allocation of nearly constant energy of rigid translation ($E_{\rm com}$) (see supplementary material). We exclude this component from the total E in our analysis, and consider the allocation of the remaining energy $E_{\rm rel}$ to obtain a time dependent signature of each event on a lower dimensional simplex. In particular, we capture the signature generated by the following decomposition of $E_{\rm rel}$ using ensemble fibration on the 1-simplex by two different methods

(ENS-I)
$$\left(\frac{E_{\text{dem}}}{E_{\text{rel}}}, \frac{E_{\text{ens}}}{E_{\text{rel}}}\right) \in \Delta^{1}, \tag{19}$$

(ENS-II)
$$\left(\frac{E_{\text{ens.rot}}}{E_{\text{rel}}}, \frac{E_{\text{rel}} - E_{\text{ens.rot}}}{E_{\text{rel}}}\right) \in \Delta^{1}, \quad (20)$$

where $E_{\rm rel}=E-E_{\rm com}$, and $E_{\rm ens}=E_{\rm rel}-E_{\rm dem}=E_{\rm ens,rot}+E_{\rm vol}+E_{\rm ens,res}$. Similarly, a one dimensional simplex description using shape fibration may be given by two ways

(SHP-I)
$$\left(\frac{E_{\text{shp.res}}}{E_{\text{rel}}}, \frac{E_{\text{rel}} - E_{\text{shp.res}}}{E_{\text{rel}}}\right) \in \Delta^{1}, \quad (21)$$

(SHP-II)
$$\left(\frac{E_{\text{rot}}}{E_{\text{rel}}}, \frac{E_{\text{shp}}}{E_{\text{rel}}}\right) \in \Delta^{1}, \tag{22}$$

where $E_{\rm shp}=E_{\rm rel}-E_{\rm rot}=E_{\rm shp,res}+E_{\rm vol}+E_{\rm ens,res}.$ On the 1-dimensional simplex we have four different geometric ways of looking at flocking event signatures. On the 2-dimensional simplex Δ^2 one has two different signatures for each flocking event

(2DENS)
$$\left(\frac{E_{\text{dem}}}{E_{\text{rel}}}, \frac{E_{\text{ens.rot}}}{E_{\text{rel}}}, \frac{E_{\text{ens.def}}}{E_{\text{rel}}}\right) \in \Delta^2, \quad (23)$$

(2DSHP)
$$\left(\frac{E_{\text{rot}}}{E_{\text{rel}}}, \frac{E_{\text{shp.res}}}{E_{\text{rel}}}, \frac{E_{\text{ens.def}}}{E_{\text{rel}}}\right) \in \Delta^2, \quad (24)$$

corresponding respectively to the ensemble and shape fibrations. Letting E_i , i=1,2,3 stand in for fractional energy modes, one can associate an average entropy $S=\langle -\sum_{i=1}^3 E_i \log_2 E_i \rangle$ to each event (the average denoted by angle bracket $\langle \cdot \rangle$ is taken over the duration of the event). The results are shown in Figs. 1 and 2. We will refer to S as the *entropic cost*. For both SHP and ENS fiberings Event 2 has the highest entropic cost, although event-to-event variability in this measure is not very substantial. (The notion of average entropy to define entropic cost

² Δ^{k-1} denotes the (k-1) dimensional probability simplex

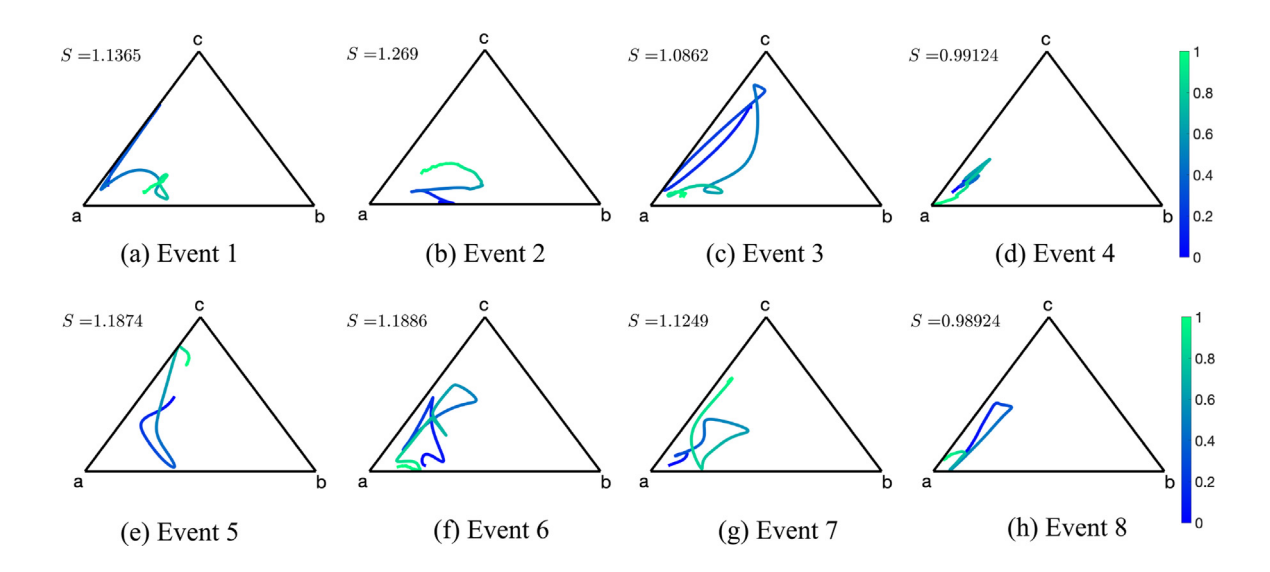


Fig. 1. Signatures on the 2-D simplex using ensemble fibering for all eight events. Each signature is colored by normalized time, with initial time in blue and final time in green. Vertices a, b and c of the simplex correspond to the kinetic energy fractions of $E_{\text{dem}}/E_{\text{rel}}$, $E_{\text{ens.rot}}/E_{\text{rel}}$ and $E_{\text{ens.def}}/E_{\text{rel}}$, and S is the entropic cost calculated for each signature in base two. Except for Event 4 which shows little variation in its allocation of E_{rel} to the democratic strategy, other events display a more complex evolution of the energy distributions to predominantly two of the components. (For interpretation of the references to color in this figure legend, the reader is referred to the web version of this article.)

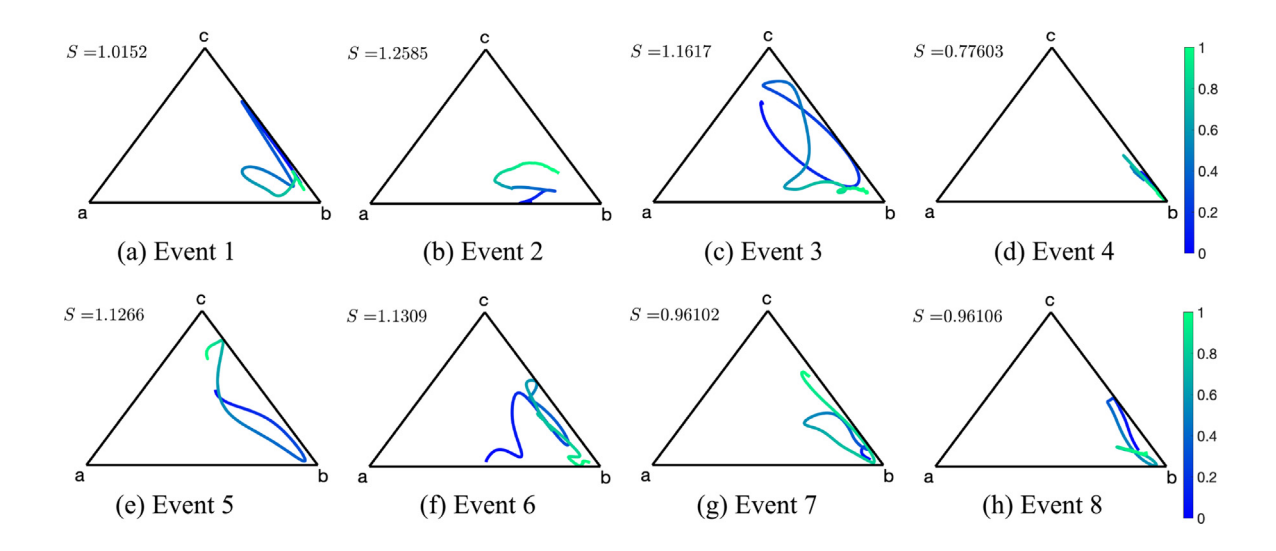


Fig. 2. Signatures on the 2-D simplex using shape fibering for all eight events. Each signature is colored by normalized time, with initialized time in blue and final time in green. Vertices a, b and c of the simplex correspond to the kinetic energy fractions of E_{rot}/E_{rel} , $E_{shp,res}/E_{rel}$ and $E_{ens,def}/E_{rel}$, and S is the entropic cost calculated for each signature in base two. Similar to the signatures corresponding to the ensemble fibering, Event 4 has the least variation in the allocation of E_{rel} almost entirely to $E_{shp,res}$ over its total duration, while other events undergo more complex evolution of the energy distributions. (For interpretation of the references to color in this figure legend, the reader is referred to the web version of this article.)

parallels that of complexity in [37] which is in part concerned with symbolic sequences over finite alphabets in the study of dance movements.)

From the formulas relating the different energy modes it follows that one can view the Δ^1 signature as a compression of the Δ^2 signature. One should note that entropic cost is not sensitive to temporal variations in the signature. By fitting suitable dynamic models to signatures, one can develop a measure that is sensitive to temporal variability. We do precisely this in Section 5, working out the details in the setting of signatures on Δ^1 . As we shall see, this also reveals fibering dependencies

of signature properties. Our approach is based on generative evolutionary game dynamics modeling the competition between the flock-scale strategies.

The moment-to-moment decisions made by individuals in a flock, taking account of the decisions by their conspecific neighbors and the predators, contribute to flock-scale strategies captured in the present section by time dependent signatures on the probability simplex. Fractional energy modes are conceptualized as probabilities defining mixed strategies in a game. This sets the stage for an evolutionary game-theoretic treatment of flocking events and quantitative comparisons of events.

5. Generative models on the simplex and the data-smoothing problem

In this work, instead of modeling the microscopic behavior of individual members of the flock that result in complex collective motion, motivated by [16], we adopt the viewpoint that the flock operates as if it is a single entity, capable of exhibiting different 'modes' of behavior. These modes or strategies are identified with the allocation of kinetic energy components. The temporal variations of a resulting signature on the probability simplex as explained in Section 4 can be captured by an underlying controlled evolutionary game that models competition between strategies. The average Hamiltonian associated to optimal controls in this setting is interpreted as a measure of cognitive cost.

Our approach in this section is informed by the concept of a three-layered cognitive hierarchy operating at multiple timescales, shown in Fig. 3, to model decision-making by the collective [24]. The bottom layer captures the interaction of the flock with its environment at a fast time-scale. This interaction is in accordance with a mixed-strategy choice determining the allocations of kinetic energy, dictated by replicator dynamics in the middle layer operating at a slower time-scale. The fitness map defining this replicator dynamics is in turn modulated by means of controls in the top layer, at the slowest time-scale. While the time-scale differences of this model are meant to distinguish reaction to fast external stimuli from long term learning, the top layer can flexibly intervene in order to accommodate for a changing environment or enable response to an adversary. With these in mind, we propose a class of generative models on the simplex.

Controlled evolutionary games offer a natural model for capturing the underlying dynamics that generates signatures representing time-dependent mixed strategies on a simplex. The replicator dynamics that captures the evolutions of fractions x_i of k types is given by

$$\dot{x} = \Lambda(x)(f(x) - \bar{f}(x)\mathbf{e}),\tag{25}$$

where $\Lambda(x) = \operatorname{diag}(x_1, x_2, \dots, x_k) \in \mathbb{R}^{k \times k}, f(x) = [f^1(x) \dots f^k(x)]^\mathsf{T} \in \mathbb{R}^k$ is a fitness map such that each component is an element of $C^\infty(\Delta^{k-1})$, the space of smooth functions on the simplex, $\bar{f}(x) = \sum_{i=1}^k x_i f^i(x)$ is the average fitness, and $\mathbf{e} = [1 \dots 1]^\mathsf{T} \in \mathbb{R}^k$. Replicator dynamics have been shown to be universal in recent work [25]. That is, every simplex-preserving dynamics can be transformed into replicator dynamics with appropriate fitness. Therefore, they are natural candidates for generative models on the simplex, as explained below.

Consider the system on Δ^{k-1} [25]

$$\dot{x} = u_1 \hat{f}_1 + u_2 \hat{f}_2, \tag{26}$$

where f_i , i = 1, 2 are fitness maps, and \hat{f}_i , i = 1, 2 are associated replicator vector fields, and u_i , i = 1, 2 are controls. Suppose the fitness maps are given by $f_1 = [a_1 \dots a_k]^T \in \mathbb{R}^k$, a constant fitness, and $f_2 = Bx$, a linear fitness map where all a_i 's are assumed to be distinct and positive, and B is assumed to be non-singular. Then, according to [24,25], (26) is controllable. This implies that there exist controls u_i , i = 1, 2 such that any two points in the interior of the probability simplex can be connected by a solution curve of (26). The dynamics (26) with the specific choice of fitness maps can be used to explain/approximate signatures on the simplex for two reasons: first, due to controllability, and second, such a system allows us to express and steer competition between the strategies. When $u_2 = 0$ and $u_1 = 1$ identically, the behavior of (26) is to converge to a pure strategy. For this reason, f_1 can be identified as dynamics due to a bias contributed by the ordering of the constant fitness components learned via games

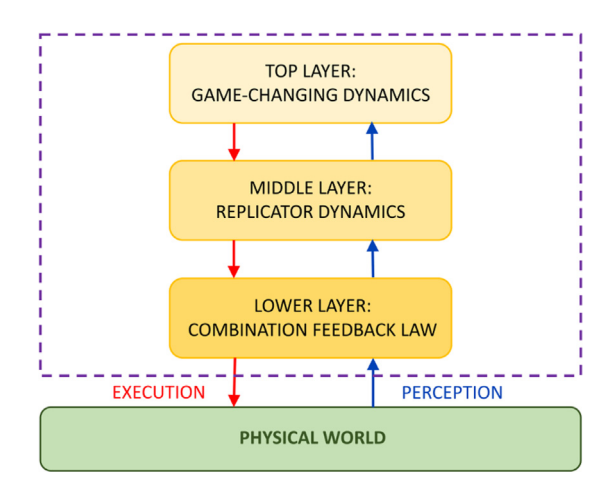


Fig. 3. The cognitive hierarchy of collective decision making. At the lowest layer, the birds of the flock interact with the environment by implementing feedback laws with respect to conspecific neighbors, predators and other stimuli. The actions of the individual birds result in a distribution of the total kinetic energy into different modes, whose evolution is captured by the replicator dynamics in the middle layer. At the top layer, the temporally changing fitness of each flock strategy is captured by the control variable.

against nature as in [38]. On the other hand, when $u_1 = 0$ and $u_2 = 1$ identically, the evolution of the strategies is influenced by the game matrix B which reflects a comparative assessment of the pure strategies when pitted against each other. Therefore, (26) is interpreted to be a system capable of producing any desired mixed strategy decision, by managing the influence of pre-existing biases and learned information or experience, with the controls as driving forces.

5.1. Specialization to k = 2

Since we are interested in describing the evolution of two flock strategies as in Eqs. (19) and (20) for ensemble fibration or Eqs. (21) and (22) for shape fibration, we capture the signature of a flocking event via a generative model on the 1-simplex. We consider an evolutionary game model, namely replicator dynamics equipped with a multiplicative control, in order to describe their evolution in the interior (0, 1) of the one-dimensional simplex. The choice of replicator dynamics is influenced by its universality in describing simplex-preserving dynamics, and by virtue of determining extremals for a variational problem [39,40]. With the inclusion of a control variable, we consider a different variational problem that aims to perform data smoothing using regularization as in [36]. To see this, let $\underline{x} = [x_1 \ x_2]^T \in \Delta^1$ where x_i , i = 1, 2 denote the prevalence of strategies i (to be specified) on the simplex with the natural constraint $x_1 + x_2 = 1$. $x_i = 1$, i = 11, 2 correspond to allocation of $E_{\rm rel}$ entirely to one of the two pure strategies. Suppose that the probabilities associated with the strategies are updated (evolved) according to the rule

$$x_i(t+1) = x_i(t) \frac{f^i(\underline{x})}{\bar{f}(\underline{x})},\tag{27}$$

where the fitness map $f(\underline{x}) = A\underline{x}$ and $\bar{f}(\underline{x}) = x_1f^1(\underline{x}) + x_2f^2(\underline{x})$. Here, $A = [a_{ij}]$ defines a payoff matrix with a_{ij} denoting the payoff of the *i*th strategy against *j*th strategy. (In the case that the payoffs do not depend on the strategy *j* against which it is matched up, the columns of *A* are identical.) In the ode limit of (27), after an

inhomogeneous time-scale change, we get the equations

$$\dot{x}_i(t) = x_i(t)(f^i(\underline{x}) - \bar{f}(\underline{x})), \quad i = 1, 2.$$
 (28)

Since addition of the same term to each component of the fitness keeps the dynamics (28) unchanged, by subtracting a_{21} and a_{12} from the first and second column elements of A respectively, we get the equivalent payoff matrix

$$\tilde{A} = \begin{bmatrix} a_{11} - a_{21} & 0 \\ 0 & a_{22} - a_{12} \end{bmatrix}. \tag{29}$$

We restrict the parameters of the matrix such that $a_{11} - a_{21} = -(a_{22} - a_{12}) = \beta$ so that the fitness can be rewritten as

$$f(\underline{x}) = \beta \begin{bmatrix} 1 & 0 \\ 0 & -1 \end{bmatrix} \underline{x}. \tag{30}$$

Due to the simplex constraint, (28) is completely described using $x = x_1$,

$$\dot{x}(t) = \beta x(t)(1 - x(t)), \tag{31}$$

with x = 0, 1 corresponding to the pure strategies 2 and 1 respectively. This allows us to adopt a time-scale change by the factor β and introduce a time-varying control to modulate the fitness as in (26) to arrive at our generative model

$$\dot{x}(t) = u(t)x(t)(1 - x(t)). \tag{32}$$

This dynamics results in asymptotic convergence to the pure strategy x=1 in the absence of temporal modulation, that is, when $u(t)\equiv 1$. However, the time-varying control u serves to model changing preferences for the flock strategies by appropriate changes in its sign and magnitude. Such a temporal modulation of the fitness ensures feasibility of capturing arbitrary signatures in the interior of the simplex.

5.2. Optimal control problem

Given a set of data points $\{x_0^d, x_1^d, \ldots, x_N^d\}$ with each $x_k^d \in (0, 1), k = 0, 1, \ldots, N$, at time instants $\{t_0, t_1, \ldots, t_N\}$, we formulate the optimal control problem

$$\min_{x(t_0), \ u(\cdot)} J(x(t_0), u) = \sum_{i=0}^{N} F_i(x(t_i)) + \frac{\lambda}{2} \int_{t_0}^{t_N} u^2(t) dt,$$
(33)

subject to: $\dot{x} = ux(1-x)$,

where the fit errors F_i 's are given by the Kullback–Leibler divergence measure of mismatch between the data and the state

$$F_i(x) = x_i^d \log \left(\frac{x_i^d}{x}\right) + (1 - x_i^d) \log \left(\frac{1 - x_i^d}{1 - x}\right), \quad i = 0, 1, \dots, N.$$
(34)

We can directly appeal to Pontryagin's Maximum Principle (PMP) and theorem 3.1 to write necessary conditions for optimality. We can write the pre-Hamiltonian as

$$H(x, p, u) = upx(1 - x) - \frac{\lambda}{2}u^{2}.$$
 (35)

The Hamiltonian maximization condition (7) yields an optimal control in each time interval $t \in (t_i, t_{t+1}), i = 0, 1, ..., N-1$,

$$u = \frac{1}{\lambda} px(1-x),\tag{36}$$

with the Hamiltonian given by

$$\mathcal{H}(x,p) = \frac{1}{2\lambda} p^2 x^2 (1-x)^2. \tag{37}$$

Hamilton's Eqs. (6) read

$$\dot{x} = \frac{1}{\lambda} p x^2 (1 - x)^2$$

$$\dot{p} = -\frac{1}{\lambda} p^2 x (1 - x) (1 - 2x).$$
(38)

The jump conditions (8) for p can be written as

 $p(t_0^-) = 0$,

$$p(t_i^+) - p(t_i^-) = \frac{x(t_i) - x_i^d}{x(t_i)(1 - x(t_i))}, \quad i = 0, 1, \dots, N,$$
(39)

Remark 5.1. Note that the optimal control is piecewise constant since $\frac{du}{dt} = 0$ for each of these time intervals $t \in (t_i, t_{i+1})$, $i = 0, 1, \ldots, N-1$. So is the PMP Hamiltonian as seen from Eqs. (36) and (37).

Therefore, denoting $x_k = x(t_k)$, k = 0, 1, ..., N, any optimal control can be described by a tuple $(u_0, u_1, ..., u_N)$ with the conditions

$$u_0 = \frac{1}{\lambda} (x_0 - x_0^d),$$

$$u_k - u_{k-1} = \frac{1}{\lambda} (x_k - x_k^d), \quad k = 1, 2, \dots, N,$$

$$u_k = 0$$
(40)

Piecewise constancy of the control input allows us to write the solution to the state Eq. (32) explicitly. Suppose the sampling time of the signature is uniform, i.e. $\Delta t := t_{k+1} - t_k$, $\forall k \in \{0, \ldots, N-1\}$, integrating the state Eq. (32) in (t_k, t_{k+1}) , we can write

$$x_{k+1} = \frac{x_k e^{u_k \Delta t}}{1 + x_k \left(e^{u_k \Delta t} - 1 \right)}, \quad k = 0, 1, \dots, N - 1.$$
 (41)

By iteration, we can in turn write every x_k as a function of x_0 and $u_0, u_1, \ldots, u_{k-1}$,

$$x_{k} = x_{k}(x_{0}) = \frac{x_{0}e^{(u_{0}+u_{1}+\cdots+u_{k-1})\Delta t}}{1+x_{0}\left(e^{(u_{0}+u_{1}+\cdots+u_{k-1})\Delta t}-1\right)}, \quad k = 1, 2, \dots, N.$$
(42)

The endpoint condition $(u_N = 0)$ can then be written as

$$g(x_0) = \sum_{k=0}^{N} (x_k - x_k^d) = 0,$$
(43)

where we use (42). Solving the optimal control problem (33) thus boils down to solving (43) for $x_0 \in (0, 1)$, constrained by (40), (41), (42).

Remark 5.2. The value of the regularization parameter λ is usually chosen through cross validation technique. We do not employ this. The value of λ is chosen such that the root finding algorithm for solving (43) converges for all events. For $\lambda=0.2$, (assuming the logarithms in Eq. (34) are natural logarithms) the roots were found with good accuracy for all events with the value of the function $g(\cdot)$ dropping to the order of 10^{-5} . For lower λ however, the problem becomes stiffer and left hand side of (43) demonstrates 'effective discontinuity' in x_0 . This poses serious problem in solving (43). As a future step, cross validation could be explored to arrive at a good value of λ in the range where (43) can be solved.

Remark 5.3. A concern with not performing cross validation to obtain the parameter λ is overfitting to noise remaining in the

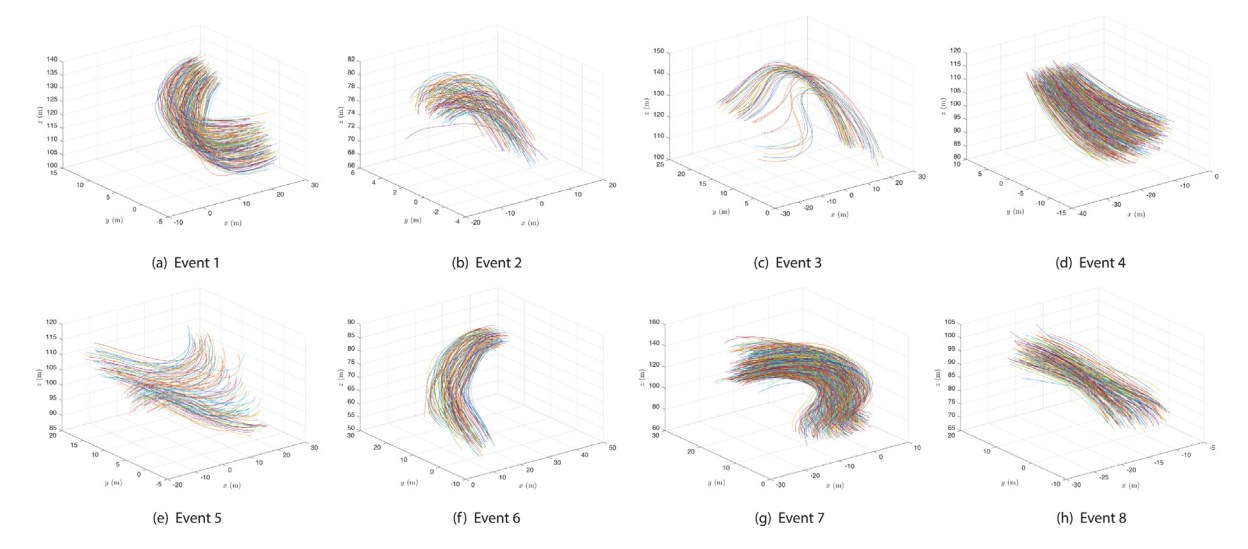


Fig. 4. Starling flight trajectories for all eight events. The time-sampled raw data was processed to generate smooth trajectories as shown here. The details for each event are given in Table 1.

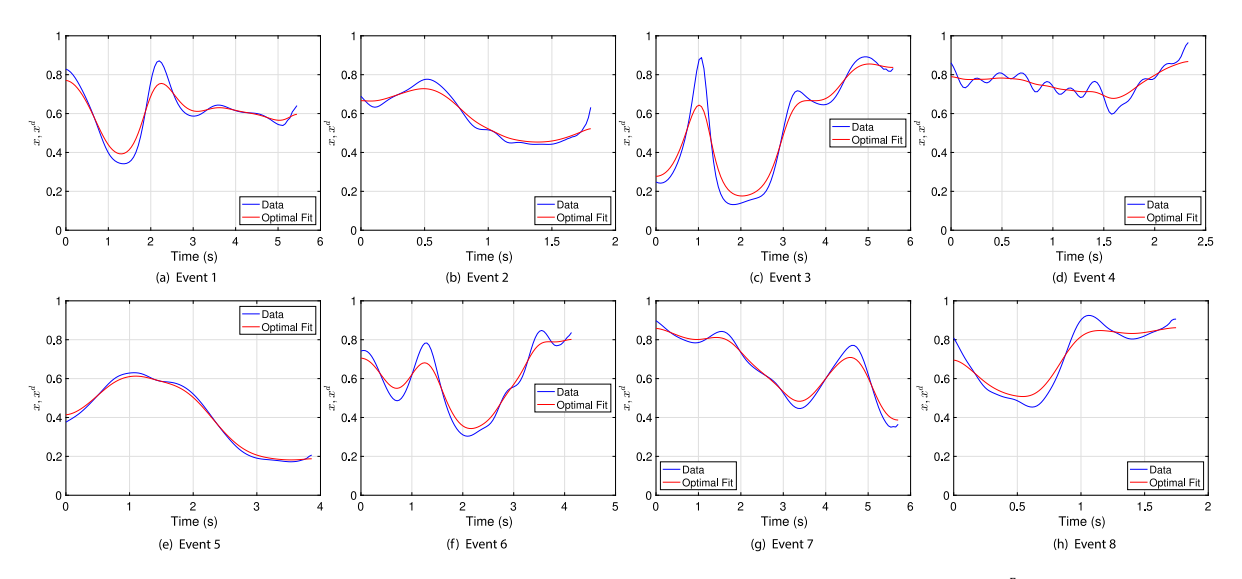


Fig. 5. Event signature and its optimal fit on the 1-D simplex, for the case ENS-I, i.e. here $x = \frac{E_{\text{dem}}}{E_{\text{res}}}$.

signature. We note here that the original flight data was subjected to data-smoothing to obtain smooth trajectories [15]. This data-smoothing process used ordinary cross validation for the trajectory of each bird to determine the appropriate weight to the regularization term. This procedure generated smooth trajectories with suppressed level of noise compared to the original data. We then construct the sampled signature $\{x_0^d, \ldots, x_N^d\}$ from these smooth trajectories. Therefore, not performing cross validation for the data smoothing on the simplex may not be deleterious, and the approach indicated in Remark 5.2 may suffice.

6. Signature fitting results and cognitive cost

For all eight events, we perform the data smoothing technique as described in Section 3.1 to obtain smooth flight trajectories. These are shown in Fig. 4. Given the smooth trajectories for all the birds in a flocking event, we compute signatures in Δ^1 and solve the optimal control problem (33) and report the results here. The value of the regularization weight λ is taken to be 0.2 and 100 signature data samples at regular time intervals are taken for all events. Given this data vector, we solve Eq. (43), constrained by

(40), (41) and (42), for $x_0 \in (0, 1)$. The MATLAB function *fzero* was used to solve the root finding problem. Control solutions for the *games* (ENS-I) (19) and (SHP-II) (22) for individual events are shown in Figs. 5 and 6, respectively. In Table 2, we report time-averaged Hamiltonian and time-averaged total costs for all the different games that we consider in Eqs. (19)–(22). The piecewise constant control signals are plotted in Figure S2 for (ENS-I) and in Figure S3 for (SHP-II) in the Supplementary material.

The mechanical activity of members of the flock in response to conspecific neighbors and any detected predators gives rise to the flock-scale behaviors we have discussed earlier. The cognitive process in each individual bird underlying such mechanical activity is not the subject of this paper. Instead we focus on flock-scale behaviors and associated (rapid) morphological changes which induce cognitive burdens (through the confusion effect) on the perceptual capabilities of a predator seeking to take a prey item from the flock. The cognitive cost of a flocking event, as discussed in this paper, is a measure of this burden. We **define** the average value of the PMP Hamiltonian of an event to be the cognitive cost. It will be shown below that this measure captures temporal variability of the signature. The time-averaged total cost J/T is also a related metric for an event. Both are graphically represented in

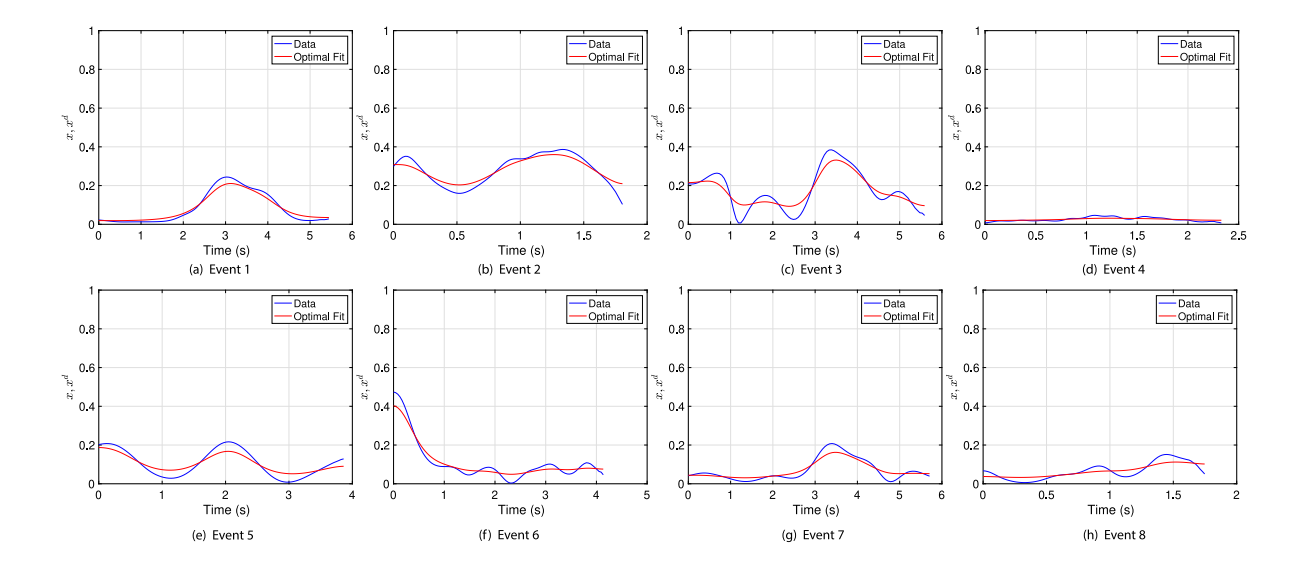


Fig. 6. Event signature and its optimal fit on the 1-D simplex, for the case SHP-II, i.e. here $x = \frac{E_{\text{rot}}}{E_{\text{ext}}}$.

Table 2Flocking event metrics: time-averaged Hamiltonian or cognitive cost and time-averaged total cost for all eight flocking events, and for all four games.

Duration (seconds)	∫ Hdt ∫dt				$\frac{J(x_0,u)}{\int dt}$			
	(ENS-I)	(SHP-I)	(ENS-II)	(SHP-II)	(ENS-I)	(SHP-I)	(ENS-II)	(SHP-II)
5.4875	0.1232	0.1263	0.0976	0.1077	0.1981	0.1975	0.1454	0.1499
1.8176	0.1432	0.1018	0.2210	0.1760	0.2227	0.1619	0.3769	0.3118
5.6118	0.2735	0.2392	0.0613	0.1073	0.4595	0.4092	0.1557	0.2495
2.3471	0.1021	0.1270	0.0107	0.0190	0.2440	0.2702	0.0594	0.0610
3.8824	0.0779	0.2699	0.1587	0.1383	0.0896	0.3692	0.3001	0.3041
4.1588	0.1809	0.1634	0.0846	0.1105	0.2799	0.2706	0.2063	0.2090
5.7353	0.0804	0.1293	0.0576	0.0619	0.1127	0.2079	0.1087	0.1221
1.7588	0.4569	0.4069	0.0731	0.1090	0.8037	0.8361	0.2074	0.3810

Fig. 7, for each of the 4 distinct geometric ways (or games) of looking at flock event signatures on the 1-dimensional simplex.

As seen from Table 2 and Fig. 7, the trend of (ENS-I) closely follows that of the game (SHP-I), except for Event 5. The trend of (ENS-II) closely follows that of (SHP-II), without making an exception of Event 5. Thus we see that there is a pairing of games in the 1-dimensional simplex in the information they yield about events. Now referring to Figs. 1 and 2, which portray signatures on the 2-dimensional simplex, note for each event, for games (2DENS) and (2DSHP) respectively, the signatures tend to allocate lower energy fractions to one of the pure strategies (vertex **b** and vertex a respectively). This suggests that analysis on the 1-dimensional simplex is sufficiently informative. An extreme situation occurs with Event 4 with signature hovering close to a pure strategy without much temporal variability (see Figs. 5 and 6). In this case, one might expect low cognitive cost (as seen in Table 2, especially in the paired games (ENS-II) and (SHP-II)). It can be seen in Figs. 1 and 2 that for this event, E_{rel} is nearly all E_{dem} and $E_{\text{shp.res}}$ respectively.

Justification for using the average PMP Hamiltonian: In looking at plots of control signals (as in Figure S2 for (ENS-I) and Figure S3 for (SHP-II)) one needs to be mindful that short duration peaking of controls is not by itself indication of high temporal variability of signature overall. One might expect that high average absolute value of control flags an event as costly. But we have a different and more natural choice. Observe that the reconstructed signatures (in red, which track the empirical signatures in blue in

Figs. 5 and 6) satisfy the model (32), with control u(t) taking piece-wise constant values u_i obtained from PMP in intervals (t_i, t_{i+1}) , i = 0, 1, 2, ..., N-1 (as Section 5). While in each such interval \dot{x}^2 is proportional to u_i^2 , a measure of temporal variability of the reconstructed signature over the duration of the event is given by the substitution of the PMP control values into the penalty term in (33). From (36) and (37) this is simply

 $N \times (average PMP Hamiltonian)$.

Thus we see that the average PMP Hamiltonian is a suitable scalar measure of temporal variability of flock signature and of use in ordering the events – answering the **question** raised in the Introduction. In this regard Event 8 and Event 3 stand out in paired games (ENS-I) and (SHP-I) – see Table 2 and Fig. 7. The paired games (ENS-II) and (SHP-II) draw attention to Event 2 and Event 5 – see Table 2 and Fig. 7.

As already discussed in Section 4 in the setting of the 2-dimensional simplex, where we associate an entropic cost *S*, the *empirical* entropic cost for the setting of the 1-dimensional simplex can be computed as

$$S = \frac{1}{N} \left(-\sum_{i=0}^{N} \left(x_i^d \log_2 x_i^d + \left(1 - x_i^d \right) \log_2 \left(1 - x_i^d \right) \right) \right). \tag{44}$$

The plots of normalized cognitive cost obtained from the smoothed trajectory on the simplex and time-averaged entropy based on the raw signatures on the simplex for all eight events are depicted in Fig. 8. We observe that for ENS-II and SHP-II the

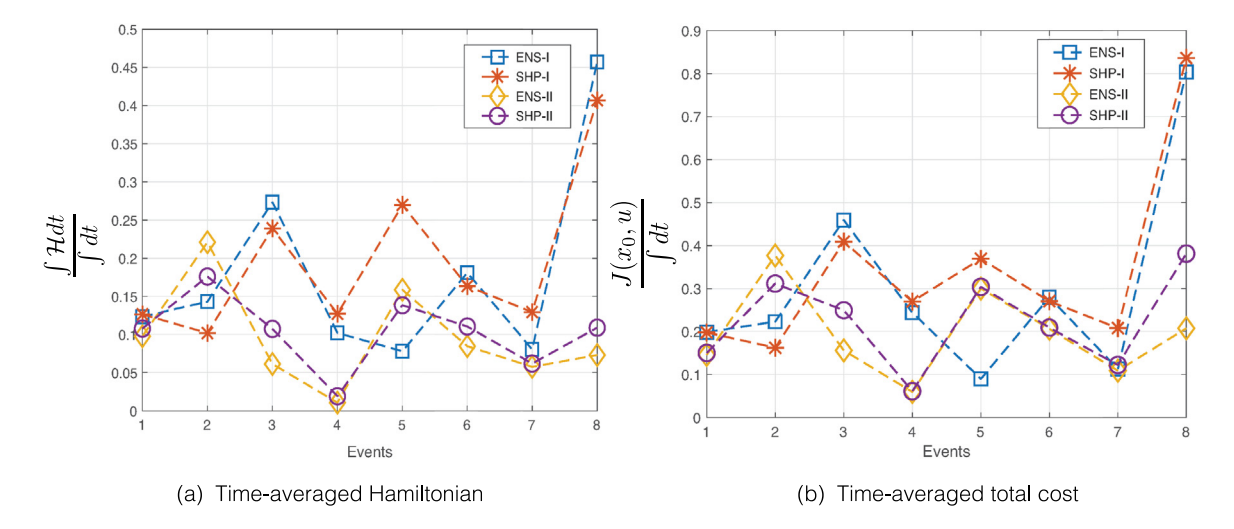


Fig. 7. Comparisons of flocking event metrics across all four games in 1-simplex: (a) time-averaged Hamiltonian or cognitive cost, (b) time-averaged total cost.

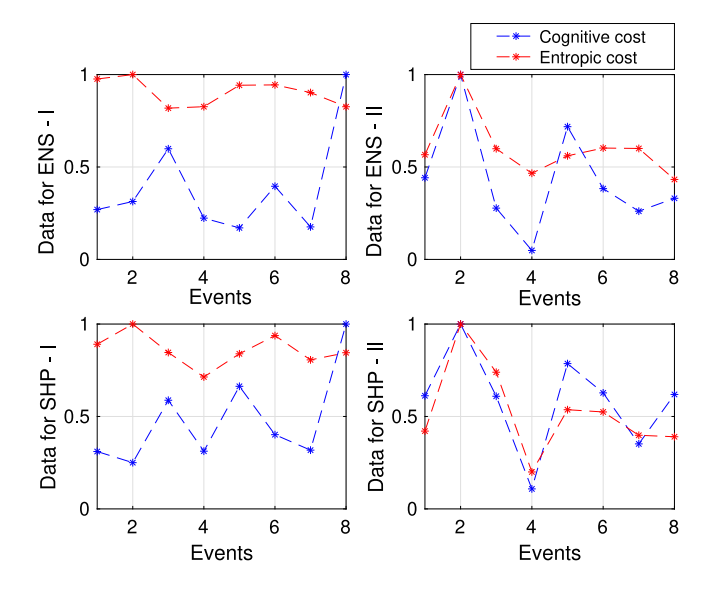


Fig. 8. Plot of normalized (by maximum across all eight events) cognitive cost (blue) against entropic cost (red) for all four games. (For interpretation of the references to color in this figure legend, the reader is referred to the web version of this article.)

entropic cost and the cognitive cost appear to show consistent trends. Such is not the case with the other games (ENS-I) and (SHP-I). Apparently the information obtained from entropic cost depends on the game. This may also be due to the insensitivity of entropic cost to temporal variability in signature.

7. Discussion

Distributed decision-making across a collective leads to phenomena in the large, not shaped by any one individual. In the setting of starling flocks this is exhibited in the form of flock-scale behaviors (emerging from individuals interacting with conspecific individuals and predators), recognizable as morphological changes over time, and quantified as dynamic allocations of kinetic energy modes. The different energy modes, defined here by appeal to geometric decompositions, are thought of as pure

strategies of a controlled evolutionary game with the fitness modulated by time-varying decision or control variables. From empirical data on trajectories of individuals in a flocking event, further compressed into event signatures on the probability simplex where mixed strategies of the game reside, these controls are found by solving an optimal control problem to best-fit the signatures. The Pontryagin Maximum Principle (PMP) is used for this computation. The time-averaged PMP Hamiltonian, defined as the cognitive cost of the event, is a measure of the cognitive burden on the perceptual capabilities of a predator seeking to take a prey item from the flock. In the basic two mode version of the problem (on the one dimensional simplex) the formulation of the optimal control problem makes the cognitive cost track the temporal variability of the reconstructed signature – higher the variability higher is the cost.

We suggest that higher cognitive cost of an event signature is an indicator of rapid morphological changes to the flock as perceived by a predator, hence magnifying the confusion effect experienced by the predator and leading to lowered success rate in capturing prey in the flock. This is supported by the results of Section 6. We have also argued that another measure, the entropic cost, interpretable as how uncertain the behavior of the flock appears to be to an observer (predator), also offers some clues, despite the fact that it is insensitive to temporal variation. In the discussion of 2-dimensional simplex signatures in Section 4, the dominance of entropic cost of Event 2 draws attention to that case as potentially influenced by predator attack. This is also supported by the cognitive costs of paired games (ENS-II) and (SHP-II) in Table 2, and Fig. 8. On the other hand, data on the 1-dimensional simplex signatures collected in Table 2 highlight the dominance of cognitive cost for Event 8 in paired games (ENS-I) and (SHP-I), again a case potentially influenced by predator attack. Taken together the cost measures suggest the possibility of labeling Event 2 and Event 8 as predator attack related.

In summary, the suggested measures of cost, especially the cognitive cost, may serve the purpose of extracting environmental influences from flock behavioral data. This is a tentative proposal and should be tested further, with optimal control studies with generative models of signature on higher dimensional simplex (beyond the 1-dimensional case studied in detail in Sections 5 and 6 of this paper). One point to keep in mind is that the higher dimensional simplex offers a wealth of generative models with

multiple controls, but the time-averaged PMP Hamiltonian may still be the right notion of cognitive cost. We aim to pursue these matters in future work.

Data source

Starling flight data was obtained from the COBBS group of the Institute for Complex Systems in Rome (ISC-CNR), University of Rome "La Sapienza", led by Andrea Cavagna and Irene Giardina. Data on flocking events were captured principally by researchers, Stefania Melillo, Leonardo Parisi, and Massimiliano Viale.

CRediT authorship contribution statement

Udit Halder: Theoretical conceptualization of the cognitive cost and writing of the paper, Analyzed the smoothed starling flight data. **Vidya Raju:** Theoretical conceptualization of the cognitive cost and writing of the paper, Analyzed the smoothed starling flight data. **Matteo Mischiati:** Helped to edit the paper, Provided theoretical basis for energy mode decomposition. **Biswadip Dey:** Helped to edit the paper, Developed techniques for smoothing trajectories of birds from the sampled data. **P.S. Krishnaprasad:** Theoretical conceptualization of the cognitive cost and writing of the paper, Provided theoretical basis for energy mode decomposition, Developed techniques for smoothing trajectories of birds from the sampled data.

Declaration of competing interest

The authors declare that they have no known competing financial interests or personal relationships that could have appeared to influence the work reported in this paper.

Data availability

The authors do not have permission to share data.

Appendix A. Supplementary data

Supplementary material related to this article can be found online at https://doi.org/10.1016/j.sysconle.2023.105488.

References

- [1] M. Ballerini, N. Cabibbo, R. Candelier, A. Cavagna, E. Cisbani, I. Giardina, V. Lecomte, A. Orlandi, G. Parisi, A. Procaccini, M. Viale, V. Zdravkovic, Interaction ruling animal collective behavior depends on topological rather than metric distance: Evidence from a field study, Proc. Natl. Acad. Sci. 105 (4) (2008) 1232–1237.
- [2] M. Ballerini, N. Cabibbo, R. Candelier, A. Cavagna, E. Cisbani, I. Giardina, A. Orlandi, G. Parisi, A. Procaccini, M. Viale, V. Zdravkovic, Empirical investigation of starling flocks: a benchmark study in collective animal behaviour, Anim. Behav. 76 (1) (2008) 201–215.
- [3] A. Attanasi, A. Cavagna, L. Del Castello, I. Giardina, T.S. Grigera, A. Jelić, S. Melillo, L. Parisi, O. Pohl, E. Shen, M. Viale, Information transfer and behavioural inertia in starling flocks, Nat. Phys. 10 (9) (2014) 691–696.
- [4] A. Cavagna, D. Conti, I. Giardina, T.S. Grigera, Propagating speed waves in flocks: a mathematical model, Phys. Rev. E 98 (5) (2018) 052404.
- [5] M. Nagy, Z. Akos, D. Biro, T. Vicsek, Hierarchical group dynamics in pigeon flocks, Nature 464 (2010) 890–893.
- [6] U. Halder, Optimality, synthesis and a continuum model for collective motion (Ph.D. thesis), University of Maryland, College Park, 2019.
- [7] D.C. Krakauer, Groups confuse predators by exploiting perceptual bottlenecks: a connectionist model of the confusion effect, Behav. Ecol. Sociobiol. 36 (6) (1995) 421–429.

- [8] G. Beauchamp, Social Predation: How Group Living Benefits Predators and Prey, Elsevier, 2014.
- [9] G.D. Ruxton, A.L. Jackson, C.R. Tosh, Confusion of predators does not rely on specialist coordinated behavior, Behav. Ecol. 18 (3) (2007) 590–596.
- [10] B.G. Hogan, H. Hildenbrandt, N.E. Scott-Samuel, I.C. Cuthill, C.K. Hemelrijk, The confusion effect when attacking simulated three-dimensional starling flocks, Royal Soc. Open Sci. 4 (1) (2017) 160564.
- [11] R. Storms, C. Carere, F. Zoratto, C. Hemelrijk, Complex patterns of collective escape in starling flocks under predation, Behav. Ecol. Sociobiol. 73 (1) (2019) 1–10.
- [12] G. Hunt, A Darwinian dance, Living Bird Mag. (2013) 28-33.
- [13] A. Cavagna, I. Giardina, Bird flocks as condensed matter, Annu. Rev. Condens. Matter Phys. 5 (1) (2014) 183–207.
- [14] B. Dey, P.S. Krishnaprasad, Trajectory smoothing as a linear optimal control problem, in: Proceedings of Allerton Conference, Urbana-Champaign, IL, 2012, pp. 1490–1497.
- [15] B. Dey, Reconstruction, analysis and synthesis of collective motion (Ph.D. thesis), University of Maryland, College Park, 2015.
- [16] M. Mischiati, P. Krishnaprasad, Geometric decompositions of collective motion, Proc. R. Soc. A 473 (2200) (2017) 20160571.
- [17] E.B. Wilson, J.C. Decius, P.C. Cross, Molecular Vibrations: The Theory of Infrared and Raman Vibrational Spectra, Dover Publications, Inc., 1955.
- [18] A. Weinstein, Normal modes for nonlinear Hamiltonian systems, Invent. Math. 20 (1) (1973) 47–57.
- [19] R.G. Littlejohn, M. Reinsch, Gauge fields in the separation of rotations and internal motions in the n-body problem, Rev. Modern Phys. 69 (1) (1997) 213.
- [20] J. Nash, Non-cooperative games, Ann. of Math. (1951) 286-295.
- [21] J. Maynard Smith, G.R. Price, The logic of animal conflict, Nature 246 (5427) (1973) 15.
- [22] P.D. Taylor, L.B. Jonker, Evolutionary stable strategies and game dynamics, Math. Biosci. 40 (1–2) (1978) 145–156.
- [23] J. Maynard Smith, Evolution and the Theory of Games, Cambridge University Press, 1982.
- [24] V. Raju, Cognitive control, evolutionary games, and Lie algebras, (Ph.D. thesis), University of Maryland, College Park, 2019.
- [25] V. Raju, P. Krishnaprasad, Lie algebra structure of fitness and replicator control, 2020, arXiv preprint arXiv:2005.09792.
- [26] L.S. Pontryagin, V.G. Boltyanskiy, R.V. Gamkrelidze, E.F. Mishchenko, Mathematical Theory of Optimal Processes, Interscience, 1962.
- [27] S.T. Christie, P. Schrater, Cognitive cost as dynamic allocation of energetic resources, Front. Neurosci. 9 (2015) 289.
- [28] T. Egner, The Wiley Handbook of Cognitive Control, Wiley-Blackwell, Oxford, 2017.
- [29] D.G. Rand, D. Tomlin, A. Bear, E.A. Ludvig, J.D. Cohen, Cyclical population dynamics of automatic versus controlled processing: An evolutionary pendulum, Psychol. Rev. 124 (5) (2017) 626.
- [30] R. Brockett, Notes on the control of the Liouville equation, in: F. Alabau-Boussouira, et al. (Eds.), Control of Partial Differential Equations, in: Chapter 2, vol. 2048, Springer, 2012, pp. 101–129.
- [31] M.M. Nice, Edmund selous: An appreciation, Bird-Banding 6 (3) (1935) 90–96
- [32] E. Selous, Bird Life Glimpses, G. Allen, 1905.
- [33] C.H. Brighton, L.N. Kloepper, C.D. Harding, L. Larkman, K. McGowan, L. Zusi, G.K. Taylor, Raptors avoid the confusion effect by targeting fixed points in dense aerial prey aggregations, Nature Commun. 13 (1) (2022) 1–13.
- [34] G.R. Martin, Through birds' eyes: insights into avian sensory ecology, J. Ornithol. 153 (1) (2012) 23-48.
- [35] N.E. Leonard, S.A. Levin, Collective intelligence as a public good, Collect. Intell. 1 (1) (2022) 1–18.
- [36] B. Dey, P. Krishnaprasad, Control-theoretic data smoothing, in: 53rd IEEE Conference on Decision and Control, IEEE, 2014, pp. 5064–5070.
- [37] J. Baillieul, K. Özcimder, The control theory of motion-based communication: Problems in teaching robots to dance, in: 2012 American Control Conference, IEEE, 2012, pp. 4319–4326.
- [38] E. Wei, E.W. Justh, P. Krishnaprasad, Pursuit and an evolutionary game, Proc. R. Soc. A 465 (2105) (2009) 1539–1559.
- [39] Y.M. Svirezhev, Optimum principles in genetics, in: Studies on Theoretical Genetics, 1972, pp. 86–102.
- [40] V. Raju, P. Krishnaprasad, A variational problem on the probability simplex, in: 57th IEEE Conference on Decision and Control, IEEE, 2018, pp. 3522–3528.

Flocks, Games, and Cognition: A Geometric Approach

Udit Halder¹, Vidya Raju², Matteo Mischiati³, Biswadip Dey⁴, and P. S. Krishnaprasad^{5,6}

¹Coordinated Science Laboratory, University of Illinois, Urbana-Champaign, IL 61801, USA

²John A. Paulson School of Engineering and Applied Sciences, Harvard University, MA 02138, USA

³Independent Researcher, Ashburn, VA 20147, USA
 ⁴Siemens Corporation, Technology, Princeton, NJ 08540, USA
 ⁵Institute for Systems Research and ⁶Department of Electrical and Computer Engineering, University of Maryland, College Park, MD 20742, USA

1. Supplementary Material

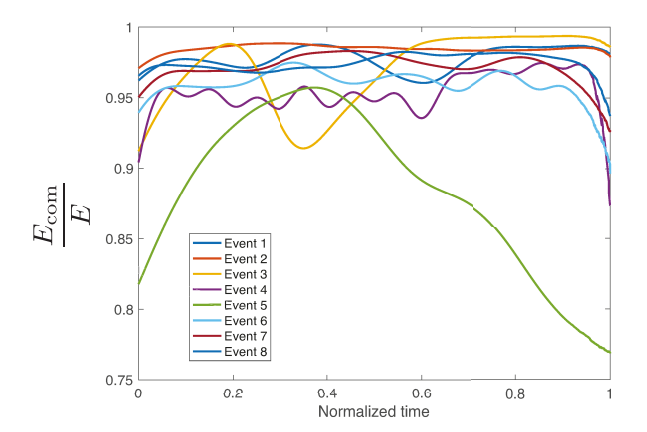


Figure S-1: The fractions of the translational energy $E_{\rm com}$ to the total kinetic energy E for all eight events. These indicate $E_{\rm com}$ is indeed the dominating part of the kinetic energy.

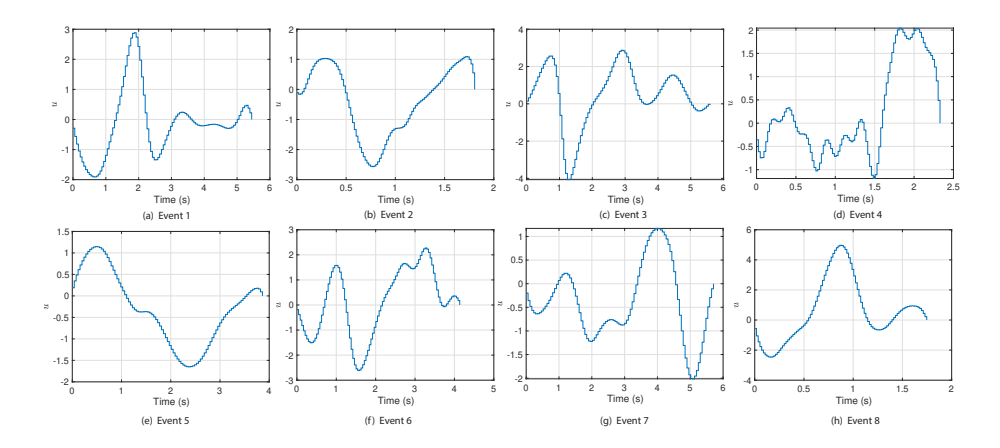


Figure S-2: Optimal Controls to fit the energy signatures on the 1-D simplex for the case $\operatorname{ENS-I}$

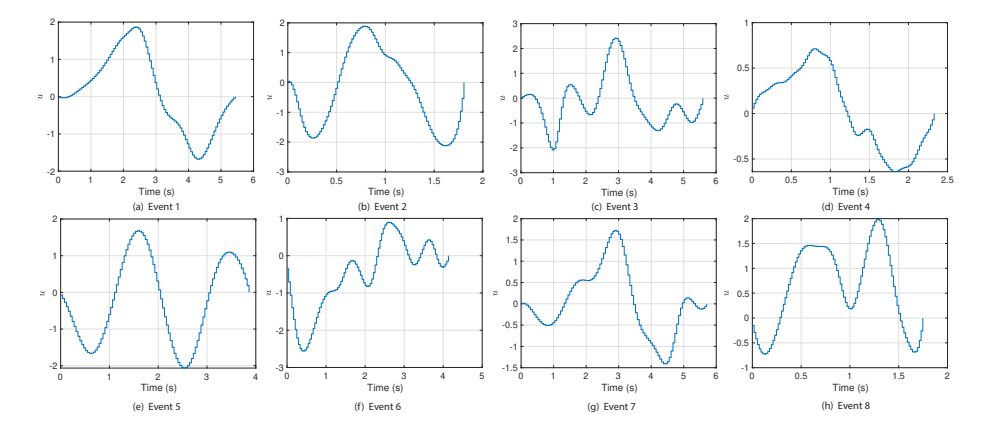


Figure S-3: Optimal Controls to fit the energy signatures on the 1-D simplex for the case SHP-II